Research Article

Journal of RAMAN SPECTROSCOPY

Received: 9 August 2010 Accepted: 6 January 2011 Published online in Wiley Online Library: 6 April 2011

(wileyonlinelibrary.com) DOI 10.1002/jrs.2908

About the SDS inclusion in PDMS/TEOS ORMOSIL: a vibrational spectroscopy and confocal Raman scattering study

A. R. Paschoal,[a]* A. P. Ayala,[a] R. C. F. Pinto,[a] C. W. A. Paschoal,[b] A. A. Tanaka,[c] J. S. Boaventura Filho[d] and N. M. José[d]

Organically modified silicates (ORMOSILs) are attractive materials due to their vast applicability and easy synthesis. The doping of these materials with sodium dodecyl sulfate (SDS) is interesting in the search for good protonic conductors. The inclusion of different concentrations of SDS in ORMOSIL membranes is investigated in the present work using Raman and infrared spectroscopy, confocal Raman microscopy and confocal imaging microscopy. The spectroscopic measurements allow us to assign the vibrational modes to the chemical groups of the structures of SDS and ORMOSIL. Furthermore, these measurements show that these materials are composites, as no interactions are observed between the SDS and the ORMOSIL matrix. The confocal Raman and confocal imaging techniques are useful to study qualitatively the SDS insertion on the surface of ORMOSIL. It was observed that the SDS sizes are very nonuniform.

Keywords: organically modified silicates; Raman; infrared; confocal; protonic conductors

Introduction

In recent years, mainly after the work of Schmidt,[1] the organic–inorganic hybrids ORMOSILs (ORganically MOdified SILicates) have attracted much attention due to their vast applicability and simple synthesis. In these compounds, the inorganic and organic phases form chemical bonds and the ORMOSILs are based on the incorporation of the oligomer and polymer species into an inorganic matrix constituted primarily by Si–O–Si networks. They have been employed in several applications, especially optical applications, due to their transparency, such as hard coatings,[2–5] waveguides and high near-IR transmission materials,[6] and gradient refractive index (GRIN) materials,[7] among others. The good reviews presented by Mackenzie and Bescher[5] and Schmidt[8] and references therein relate several other applications. The applications of these materials can also be widened because they can be synthesized using the sol-gel technique, as these materials can provide both molecular accessibility and rapid mass transport via diffusion due to their structure constituted by nanometer-sized particles surrounded by a continuous mesoporous volume.[9]

This synthesis type also permits the employment of ORMOSILs as the hosts for the incorporation of high amounts of several compounds, such as high conductivity materials. The doping with a high conductivity material is interesting in the search for good protonic conductors, which can be employed, among other applications, in protonic electrolyte membrane (PEM) fuel cells.[10–13] Thus, small molecules that show high protonic conductivity (0.02–0.1 S cm^{-1}) at room temperature, such as sodium dodecyl sulfate (SDS), phosphotungstic acid (PWA) and silicotungstic acid (SWA), have been used for doping ORMOSIL membranes. However, the use of these compounds in commercial devices is limited by the thermal and mechanical properties criteria. Recently, Pinto *et al*.[13] showed that the SDS inclusion in ORMOSIL based on poly(dimethilsiloxane) (PDMS) and tetraethoxysilane (TEOS) increases the conductivity. However, this increase was limited by the higher porosity induced in the membranes by SDS inclusion, which is more than 20%. In this work, we investigated the SDS distribution in PDMS/TEOS ORMOSIL using confocal Raman measurements in order to understand the inclusion of SDS into the membranes.

Experimental

PDMS supplied by Dow Corning, with a number-averaged molecular weight of 2200 $gmol^{-1}$, TEOS from Aldrich and SDS from Qeel were used as the raw materials to obtain the ORMOSIL membranes. Isopropanol from Vetec and dibutyl tin dilaurate from Aldrich were used as the solvent and catalyst, respectively. The pure PDMS/TEOS compound, without SDS inclusion, was synthesized by the hydrolysis and condensation of PDMS and TEOS, using a mass ratio of 70 : 30. For the SDS-containing membranes, the SDS conductor was added to the matrix in different mass (with

* *Correspondence to: A. R. Paschoal, Departamento de Física, Universidade Federal do Ceará, Campus do Pici, 60455-760, Fortaleza, CE, Brazil. E-mail: paschoal@ufma.br*

a *Departamento de Física, Universidade Federal do Ceará, Campus do Pici, 60455-760, Fortaleza, CE, Brazil*

b *Departamento de Física - CCET, Universidade Federal do Maranhão, Campus do Bacanga, 65080-040, São Luís, MA, Brazil*

c *Departamento de Química, Universidade Federal do Maranhão, 65085-580, São Luis, MA, Brazil*

d *Departamento de Físico Química, Universidade Federal da Bahia, 40170-115, Salvador, BA, Brazil*

relation to the TEOS) ratios, namely 5, 10, 20 and 30%, near the gel point. After that, the modified membranes were allowed to dry at room temperature for 7 days in Teflon® molds. Finally, the obtained membranes were dried in vacuum for 2 days. The sample thicknesses obtained were 1.204 mm (0%), 0.972 mm (5%), 1.575 mm (10%), 1.081 mm (20%) and 1.196 (30%).

The Raman scattered signal was obtained in the backscattering configuration with a Horiba iHR 550 spectrometer equipped with a Synapse charge-coupled device (CCD) system. The 632.8 nm line of a He–Ne laser operating at 50 mW was used to excite the signal.

The infrared spectra were measured using a Nicolet spectrometer Model Nexus 470 in the mid-IR range. The spectrometer was equipped with an Ever-GLO source, a KBr beamsplitter and a deuterated triglycine sulfate (DTGS) detector. In order to obtain the spectra, we used the attenuated total reflection (ATR) method through an Avatar multibounce HATR sampler.

The confocal Raman spectra and the confocal images were acquired with an alpha 300 system microscope (Witec, Ulm, Germany), equipped with a highly linear (0.02%) piezo-driven stage and an objective lens from Nikon (100×, NA = 0.9). A Nd:YAG polarized laser (λ = 532 nm) was focused to a diffraction-limited spot size (0.61λ/NA) and the Raman light was detected by a high-sensitivity, back-illuminated spectroscopic CCD located behind a 600 grooves/mm grating. The spectrometer used was an ultrahigh throughput Witec UHTS 300 instrument (70% throughput), designed specifically for Raman microscopy. The integration time for the Raman spectroscopic images was 2 s per point with steps of 0.25 μm.

Results and Discussions

In order to investigate the SDS distribution in PDMS/TEOS ORMOSIL membrane, we performed first the Raman and FTIR measurements on the samples. Figure 1 shows the main parts of the infrared spectra for the five investigated samples, together with the infrared spectra of pure SDS. It can be noted in this figure that all the infrared spectra, referred to different SDS concentrations, are very similar to each other.

The SDS inclusion in the pure membranes is observed only through the appearance of a mode at 1217 cm^{-1} (indicated by an arrow in Fig. 1(a) and (b)). This peak is characteristic of the S=O bond present in the SDS molecule and is not observed in the pure membrane. In Fig. 1(a), we also observe four bands at 662, 673, 685 and 701 cm^{-1}, which are associated with the PDMS skeletal chains. The CH_2 rocking observed at 722 cm^{-1} is very weak. This peak is slightly more evident in membranes that contain SDS, since this radical is more abundant in SDS than in TEOS. The symmetric Si–O–Si stretching is observed at 783 and 802 cm^{-1}. The last mode can be also associated with CH_3 rocking. The mode observed at 848 cm^{-1} is a Si–CH_3 deformation. The Si–OH stretching mode is observed at 1007 cm^{-1}. The presence of this bond with the OH^- group considerably affects the conductive properties of the membranes (the work involving this dielectric characterization is still in progress and will be published soon). The peak observed at 1078 cm^{-1} is related to the asymmetric Si–O–Si stretching. The band at 1257 cm^{-1} is related to an asymmetric deformation of the Si–CH_3 bond. The scissor modes of the CH_2 group are observed at 1398 and 1412 cm^{-1}. The asymmetric deformation of the CH_3 is observed at 1448 cm^{-1}. Finally, the C–H modes are observed at 2850, 2915 and 2960 cm^{-1} (see Fig. 1(c)). All these mode assignments are made on the basis of previous works.[14–17]

In Fig. 2, we show the Raman spectra of the five investigated samples. In these spectra, the SDS inclusion is clear. Thus, we can see the SDS inclusion in the pure sample by the peaks at 890, 920, 1130, 1295 cm^{-1} and the new ν(C–H) band at 2900 cm^{-1} (all indicated by dashed arrows in Fig. 2). The SDS inclusion can be correlated with the relative intensity of the bands as compared to that of the bands originating from the ORMOSIL matrix. Thus, the increase in the SDS concentration can be viewed by comparing the intensities of the bands at 890 and 920 cm^{-1} with that at 710 cm^{-1} and the intensity of the bands observed at 1130 and 1295 cm^{-1} with that observed at 1410 cm^{-1}. As we can see, the relative intensities tend to increase with the SDS concentration, as expected. Another clear indication of the presence of the SDS is found in the bands around 1070 cm^{-1} assigned to the $\nu_{as}(OSO_3)$.[16] From Fig. 2(c), one can note that the intensity of these vibrational modes increases with the SDS concentration.

The other modes are similar to those observed in the infrared spectra, with exception of the low wavenumber modes associated with the inorganic lattice. The assignments of the main observed Raman bands are shown in Table 1.

It was not possible to infer clearly about the bonding between the SDS and the pure membrane. The shift to lower wavenumbers of the peaks assigned to the stretching vibrations is one of the signatures of the hydrogen bonds and we focus on this feature in the following discussion. The bands found at 1130 and

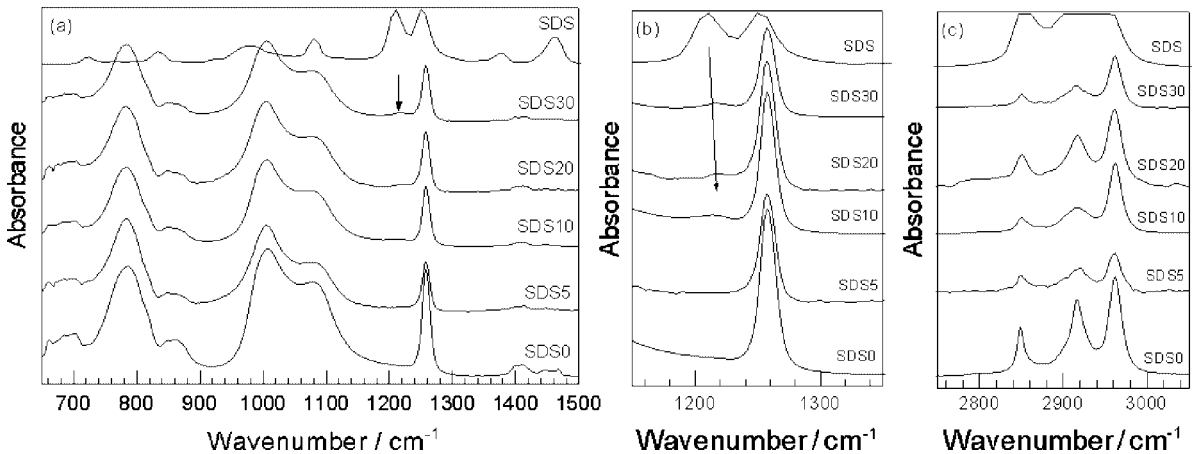

Figure 1. Infrared spectra of the several samples.

Journal of RAMAN SPECTROSCOPY

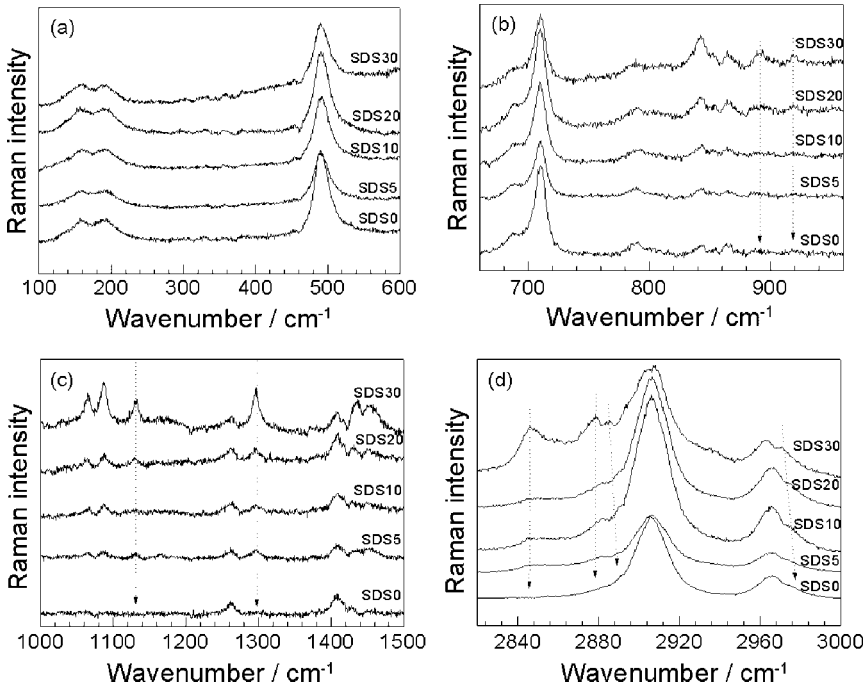

Figure 2. Raman spectra observed for the ORMOSIL PDMS/TEOS/SDS at several concentrations investigated in the four wavenumber ranges of interest.

Table 1. Raman modes observed in the ORMOSIL PDMS/TEOS with SDS at several concentrations, with their respective assignments

Mode number	SDS concentration (%)					Assignments
	0	5	10	20	30	
1	156	157	157	156	155	Skeletal siloxane
2	193	193	193	193	194	Skeletal siloxane
3	488	490	491	489	490	Tetrasiloxane ring
4	496	503	503	496	499	
5	689	688	688	689	689	C–Si skeletal
6	710	710	710	710	710	ρ (CH_2)
7	791	789	791	789	788	ν_s(Si–O–Si) or ρ (CH_3)
8	–	806	808	807	811	
9	843	842	843	842	842	δ(Si–CH_3)
10	853	853	853	853	853	ν(Si–CH_3)
11	865	866	865	866	866	PDMS (Si–CH_3)
12	–	889	893	892	892	δ(CH_2)
13	–	921	920	919	921	ν_s(Si–OH)
15	–	1061	1062	1063	1065	ν(S=O)
16	–	1088	1088	1088	1087	
17	–	1130	1129	1130	1131	
19	1262	1262	1261	1262	1261	δ_s(CH_3)
20	–	1297	1298	1296	1297	ν (S–O)
21	1409	1409	1409	1408	1408	CH_2 scissor
22	1429	1435	1429	1431	1435	
23	1457	1455	1455	1455	1456	δ_a(CH_3)
24	–	–	–	–	2846	ν(C–H)
25	–	2851	2852	2851	2857	
26	2879	2879	2879	2879	2878	
27	2906	2906	2906	2906	2906	
28	–	2936	2914	2914	2936	
29	2965	2966	2965	2965	2962	
30	2976	–	2977	2976	2970	

1295 cm^{-1} are assigned to the symmetric (ν_1) and asymmetric (ν_3) O–S–O stretching, respectively.[18] Considering the Raman spectra (Fig. 2(c)), a dislocation of these bands due to the bonding S=O···H between SDS and the ORMOSIL membrane was expected. However, as we can see, for all doped samples these vibrational modes remain unaltered, indicating that inclusion of the SDS molecule in the PDMS/TEOS ORMOSIL is purely a physical effect. In addition, the wavenumber of the peak around 1070 cm^{-1} also remains unchanged, reinforcing the suggestion of physical inclusion. It is also worth commenting that, depending on the way the SDS block is linked to the pure membrane, most of the collected light can originate from the scattering of the bulk SDS so that it is not possible to observe the lowering of the wavenumbers of the Raman peaks. Regarding this comment, the use of confocal microscopy in the second part of this article will be helpful.

In order to investigate the SDS distribution in PDMS/TEOS ORMOSIL samples, we monitored the intensity of the 1080 cm^{-1} Raman band. The images thus obtained in a sample region of 7 × 7 μm are presented in Fig. 3. In Fig. 3(a) we show an optical view of the 10% doped membrane surface and in Fig. 3(b) we show the Raman mapping of the SDS distribution in PDMS/TEOS ORMOSIL sample. In this figure, the yellow parts indicate the SDS distribution. The calculated surface area of the grains indicated by 1 and 2 in Fig. 3(a) was about 3.3 and 4.5 μm^2. As we can see, the SDS crystallite sizes are very nonuniform. This behavior was observed for all doped samples. Besides, the correspondence between Fig. 4(a) and (b) indicates that the presence of the SDS in the PDMS/TEOS ORMOSIL sample is only physical, in accordance with the results of the spectroscopic analysis.

Aiming to study the space occupied by an SDS crystallite, we carried out several depth measurements in the 30% SDS-doped PDMS/TEOS ORMOSIL. These measurements consisted of acquiring many images of 25 × 25 μm (256 × 256 points) in different confocal planes, with steps of 0.5 μm into the sample. The most important images for our discussion are shown in Fig. 4, where we

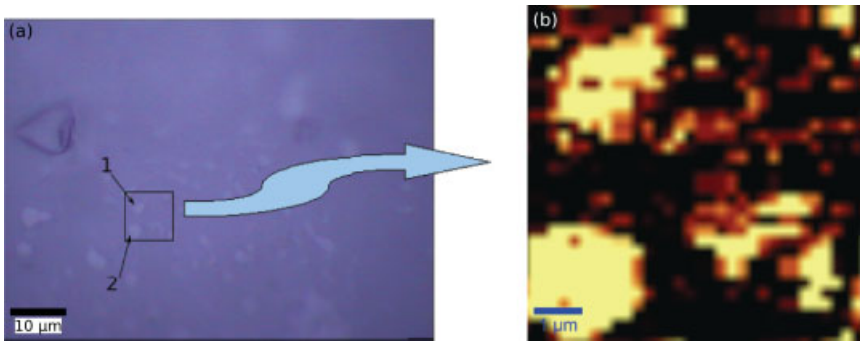

Figure 3. (a) Optical surface of the 10% SDS-doped PDMS/TEOS ORMOSIL samples obtained with a 100× lens; (b) 1080 cm^{-1} Raman band intensity mapping.

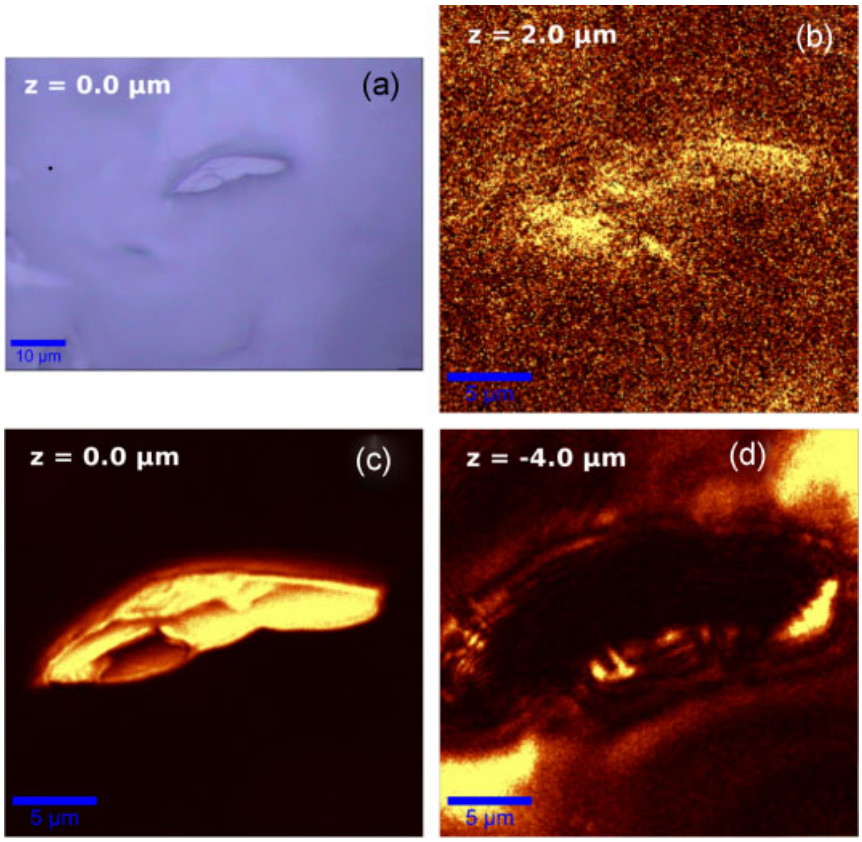

Figure 4. (a) Optical image from the surface of the 30% SDS-doped ORMOSIL membrane. (b–g) Confocal Raman images obtained for several different planes of the 30% SDS-doped ORMOSIL membrane.

obtained a profile of the SDS crystallite in the membrane. Just for reference, we consider the image observed in Fig. 4(a) as $z = 0$, with the positive direction outward from the sample. After setting this reference plane, we moved our objective lens 5 μm up and then started the confocal measurements as described above. The first acquired image was homogeneous and thus it was important to guarantee that at this height (5 μm) the contribution of the SDS block to the image acquisition was negligible. Several other images were measured in lower confocal planes, but the first indication of the presence of the SDS block was observed only at $z = 2$ μm, as can be seen in Fig. 4(b). This image does not outline the shape of the SDS block very well, but at $z = 0$ μm this is clearly achieved, as shown in the next image of the series (Fig. 4(c)). This well-defined image was already expected, since it was our starting point. We then continued our measurements by imaging confocal planes below $z = 0$ μm and hence the trend for the subsequent images is that the SDS block shape becomes undefined while other parts of the sample surface fall in the focal plane of our objective lens. This expectation is confirmed in Fig. 4(d). Finally, the last image was acquired at $z = -11.5$ μm and it was homogenous, with no indication of the presence of the SDS block, similar to the first one at $z = 5$ μm. The homogeneity of this last image is a sign that $z = -11.5$ μm is an appropriate position to stop these depth measurements. With the help of Fig. 4, we can evaluate the area of this SDS block at about 140 μm^2. The z-profile evolution presented in the images of Fig. 4 is also helpful for studying the surroundings of the SDS block. In this sense, for this investigated SDS, we observe that the heights of diagonally opposite corners

Journal of RAMAN SPECTROSCOPY

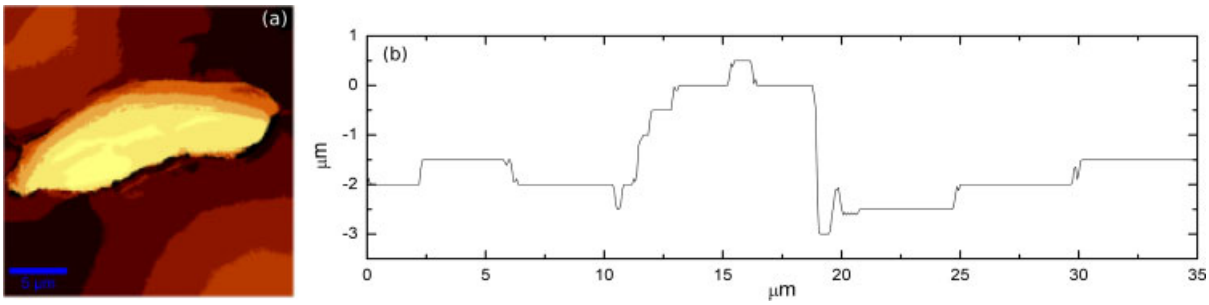

Figure 5. (a) *z*-position of the most intense confocal planes of the depth measurements shown in Fig. 4. (b) Cross section of the diagonal upper-left bottom-right.

are approximately the same (Fig. 4(d)). For completeness, it is also important to estimate the height of the SDS. In order to accomplish this, we believe that a more precise analysis can be made if we consider not only the selected images shown in Fig. 4 but all the several confocal images of this stack depth measurement together. This concise representation can be seen in Fig. 5(a), which traces a volumetric profile of the SDS crystallite. This figure is constructed by the *z* position of the highest intensity plane of each (*x*,*y*) point of the region investigated. Figure 5(b) is the diagonal cross section upper-left bottom-right of Fig. 5(a) and it can be observed that the height of the SDS is about 2.5 µm. This crystallite, therefore, is much bigger than the others identified, with a volume of 350 μm^3, indicating the large size and variation of the SDS distribution in PDMS/TEOS ORMOSIL. New studies regarding the size distribution effects on the conductivity of the doped membranes are in progress.

Conclusions

In summary, we applied vibrational spectroscopy and microscopy techniques to study the SDS inclusion in ORMOSIL membranes. We observed that the infrared spectra, referred to SDS concentrations ranging from 5% to 30%, are very similar. The only SDS characteristic peak found in the IR spectra was at 1217 cm^{-1}. This vibrational mode is related to the S═O bond present in the SDS compound. The Raman spectra clearly indicated the SDS inclusion by the presence of the peaks around 900, 1100 and 2900 cm^{-1}. Furthermore, we identified the Raman and IR peaks of the organic and inorganic parts of ORMOSIL and carried out the mode assignment on the basis of previous works. We did not observe any spectroscopic indication of the bonding between the SDS and the ORMOSIL, and this an evidence that the SDS inclusion is only physical.

Using the confocal Raman technique, we made a spectroscopic image of the SDS peak located at 1080 cm^{-1}. This image showed that the SDS crystallite sizes are very nonuniform. The contrast in the confocal Raman spectroscopic images also suggested a physical inclusion of the SDS in the ORMOSIL membranes. Confocal depth measurements allowed us to trace a volumetric profile of the SDS in the 30% doped ORMOSIL. With the help of this profile, we concluded that the SDS platelet measured was approximately 2.5 µm high, with an area of 140 μm^2.

Acknowledgements

The authors acknowledge the financial support from CNPq, FINEP and FAPEMA, the Brazilian funding agencies, and the Instituto de Pesquisa, Desenvolvimento e Inovação do Estado do Ceará (IPDI) for providing the confocal Raman equipment.

References

[1] H. Schmidt, *J. Non-Cryst. Solids* **1985**, *73*, 681.
[2] J. Wen, V. J. Vasudevan, G. L. Wilkes, *J. Sol.-Gel. Sci. Technol.* **1995**, *5*, 115.
[3] W. X. Que, Y. Zhou, Y. L. Lam, Y. C. Chan, C. H. Kam, *J. Sol.-Gel. Sci. Technol.* **2001**, *20*, 187.
[4] W. X. Que, Y. Zhou, Y. L. Lam, Y. C. Chan, C. H. Kam, *Thin Solid Films* **2000**, *358*, 16.
[5] J. D. Mackenzie, E. P. Bescher, *J. Sol.-Gel. Sci. Technol.* **2000**, *19*, 23.
[6] G. D. Kim, T. B. Kim, *J. Rare Earth* **2004**, *22*, 136.
[7] H. Schmidt, P. M. Müller, H. Krug, P. W. Oliveira, in *Materials Research Society Symposium Proceedings*, (Eds: B. K. Coltrain, C. Sanchez, D. W. Schaefer, G. L. Wilkes), Material Research Society: Pittsburgh, **1996**, pp. 553.
[8] H. Schmidt, H. Wolter, *J. Non-Cryst. Solids* **1990**, *121*, 428.
[9] W. M. Aylward, P. G. Pickup, *J. Solid State Electrochem.* **2004**, *8*, 742.
[10] U. L. Stangar, B. Orel, N. Groselj, P. Judeinstein, F. Decker, P. Lianos, *Monatsh. Chem.* **2001**, *132*, 103.
[11] I. Honma, Y. Takeda, J. M. Bae, *Solid State Ion.* **1999**, *120*, 255.
[12] I. Honma, S. Hirakawa, K. Yamada, J. M. Bae, *Solid State Ion.* **1999**, *118*, 29.
[13] R. C. F. Pinto, C. W. A. Paschoal, W. Paraguassu, M. C. Carvalho Jr, A. A. Tanaka, J. Boaventura Filho, N. M. Jose, *J. Appl. Poly. Sci.* **2010**, *155*, 851.
[14] I. Simon, H. O. Mcmahon, *J. Chem. Phys.* **1952**, *20*, 905.
[15] X. C. Li, T. A. King, *J. Non-Cryst. Solids* **1996**, *204*, 235.
[16] R. P. Sperline, *Langmuir* **1997**, *13*, 3715.
[17] L. Tellez, F. Rubio, R. Pena-Alonso, J. Rubio, *Bol. Soc. Esp. Ceram. V.* **2004**, *43*, 883.
[18] D. Barnard, J. M. Fabian, H. P. Koch, *J. Chem. Soc.* **1949**, 2442.

